NUMERICAL ANALYSIS OF BLAST PRESSURE PARAMETERS ON THE BUILDING WITH AND WITHOUT WALL AS A BARRIER

NUR SYAFIQAH BINTI ABDULLAH

B. ENG(HONS.) CIVIL ENGINEERING

UNIVERSITI MALAYSIA PAHANG

UNIVERSITI MALAYSIA PAHANG

DECLARATION OF THESIS AND COPYRIGHT

Author's Full Name : <u>NUR SYAFIQAH BINTI ABDULLAH</u>

Date of Birth : <u>19 FEBRUARY 1996</u>

Title : <u>NUMERICAL ANALYSIS OF BLAST PRESSURE PARAMETERS ON</u> THE

<u>BUILDING WITH AND WITHOUT WALL AS A BARRIER</u>

Academic Session : <u>2018/2019</u>

I declare that this thesis is classified as:

☐ CONFIDENTIAL (Contains confidential information under the Official Secret Act 1997)*

☐ RESTRICTED (Contains restricted information as specified by the organization where research was done)*

☑ OPEN ACCESS I agree that my thesis to be published as online open access (Full Text)

I acknowledge that Universiti Malaysia Pahang reserves the following rights:

1. The Thesis is the Property of Universiti Malaysia Pahang
2. The Library of Universiti Malaysia Pahang has the right to make copies of the thesis for the purpose of research only.
3. The Library has the right to make copies of the thesis for academic exchange.

Certified by:

_____
(Student's Signature)
Nur Syafiqah Binti Abdullah
New IC: 960219-04-5376
Date: 17 JUNE 2019

_____
(Supervisor's Signature)
Dr. Mazlan Bin Abu Seman
Name of Supervisor
Date: 17 JUNE 2019

NOTE : * If the thesis is CONFIDENTIAL or RESTRICTED, please attach a thesis declaration letter.

STUDENT'S DECLARATION

I hereby declare that the work in this thesis is based on my original work except for quotations and citations which have been duly acknowledged. I also declare that it has not been previously or concurrently submitted for any other degree at Universiti Malaysia Pahang or any other institutions.

_____

(Student's Signature)

Full Name   : NUR SYAFIQAH BINTI ABDULLAH

ID Number   : AA15237

Date   : 17 JUNE 2019

NUMERICAL ANALYSIS OF BLAST PRESSURE PARAMETERS ON THE
BUILDING WITH AND WITHOUT WALL AS A BARRIER

NUR SYAFIQAH BINTI ABDULLAH

Thesis submitted in fulfillment of the requirements
for the award of the
B.Eng (Hons.) in Civil Engineering

Faculty of Civil Engineering and Earth Resources

UNIVERSITI MALAYSIA PAHANG

JUNE 2017

ACKNOWLEDGEMENTS

I am sincerely grateful to ALLAH "S.W.T" for giving me wisdom, strength, patience, and assistance to complete my project work. Had it not been due to His will and favor, the completion of this study would not have been achievable.

This dissertation would not have been possible without the guidance and the help of several individuals who contributed and extended their valuable assistance in the preparation and the completion of this study. I am deeply indebted to my supervisor, Dr Mazlan bin Abu Seman for his patient, guidance, comment, stimulating suggestions and encouragement which helped me in all the time of research, writing of this thesis and assistant throughout my project work.

I also like to convey thanks to the faculty (FKASA) for providing the laboratory and workshop facilities for this project. My sincere appreciation also extends to all my friends, lecturers, teaching engineers and others who provided guidance and advice, including the crucial input for my planning and findings. The guidance and support received from all were vital to the success of this research.

Especially, I would also like to address my unlimited thanks to my family for their unconditional support, both financially and emotionally throughout my studies. My deepest gratitude goes to my family for their support, patience, love, and trust during my study. Finally, I would like to thank everyone who had involved in this study either directly or indirectly

ABSTRAK

Beban letupan mungkin disebabkan oleh peledakan bahan peledak yang tinggi dan bahan kimia. Terdapat banyak peristiwa letupan yang berlaku berhampiran bangunan yang meletup sama ada kerana keganasan atau kemalangan. Ini kerana bangunan dan infrastruktur yang dibina di kawasan awam tidak direka untuk menahan beban letupan. Oleh itu, adalah penting untuk mempertimbangkan beban letupan dalam reka bentuk bangunan. Tidak ekonomikal dan realistik untuk reka bentuk bangunan dengan rintangan letupan penuh. Sekiranya beban letupan di atas bangunan, ia akan bertindak balas berbeza berbanding dengan beban biasa. Oleh itu, simulasi akan dilakukan untuk melihat profil tekanan letupan pada bangunan. Kajian ini dilakukan untuk menilai profil tekanan letupan pada keadaan dengan dinding dan tanpa dinding. Beban letupan dengan 13.6 kg (30 lbs.) Trinitrotoluena (TNT) akan digunakan dan akan disahkan dengan artikel untuk membandingkan model 3D berangka dengan uji eksperimen sebelum ia boleh digunakan untuk parameter lain. Dalam analisis berangka ini, 3 situasi akan dipertimbangkan. Pertama, letupan di ruang terbuka. Untuk letupan kedua dan ketiga di sebelah bangunan tanpa dan dengan kehadiran dinding RC sebagai penghalang masing-masing. Simulasi ini akan dilakukan menggunakan perisian ANSYS AUTODYN. Daripada simulasi, ia menunjukkan bahawa tekanan yang tinggi pada 18 kaki hampir sama dengan tekanan yang tinggi dari artikel oleh Yan et. al (2011). Untuk Yan et. al (2011) beban tekanan lampau adalah 494.4 kPa pada 4.64 msec dan beban tekanan lampau untuk medan bebas pada 18 kaki adalah 494.4 kPa pada 4.62 msec. Untuk membina dengan kehadiran tekanan letupan RC RC boleh mengurangkan kira-kira 120%. Beban tekanan lampau pada jarak henti 1219 mm (4 kaki) tanpa dinding adalah 1255.63 kPa pada 0.22 msec, manakala beban tekanan lampau dengan dinding berkurangan kira-kira 315.24 kPa pada 1.66 msec pada jarak kebarangkalian yang sama (1219 mm). Hasil keseluruhan menunjukkan bahawa dengan kehadiran dinding RC, tekanan overpressure dapat dikurangkan. Hasil berangka menunjukkan bahawa dinding RC boleh digunakan sebagai halangan untuk mengurangkan tekanan overblur.

ABSTRACT

Blast loading may result from the detonation of high explosives and chemical ammunitions. There are many blast event occurred near the building that explode either because of terrorism or accidental. This is because the building and infrastructure construct in civilian area are not design to withstand the blast load. Therefore, it is important to consider blast loads in design a building. It is not economical and realistic to design building with full blast resistance. In the event of blast load on building, it will react differently compared to normal load. In this paper, simulation will be done to observe blast pressure profile on building. This research was done to evaluate the blast pressure profile at situation with and without wall. Blast load with 13.6 kg (30 lbs.) Trinitrotoluene (TNT) will be used and will be validated with an article to compare the numerical model 3D with experimental test before it can be used for others parameters. In this numerical analysis, 3 situations will be considered. First, the blast in open space. For the second and third, blast next to the building without and with the presence of RC wall as barrier respectively. The simulation will be done using ANSYS AUTODYN software. From the simulation, it shows that the peak blast overpressure at 18 ft. is almost same with peak blast overpressure of article by Yan et. al (2011). For Yan et. al (2011) the peak blast overpressure is 494.4 kPa at 4.64 msec and peak blast overpressure for free field at 18 ft. is 494.4 kPa at 4.62 msec. For building with the presence of the RC wall blast pressure can be reduce about 120%. The blast peak overpressure at standoff distance 1219 mm (4 ft.) without wall is 1255.63 kPa at 0.22 msec, while the blast peak overpressure with wall is reduced about 315.24 kPa at 1.66 msec at the same standoff distance (1219 mm). The overall result show that with the presence of RC wall, the blast overpressure can be reduced. The numerical result show that RC wall can be used as barrier to reduced blast overpressure.

TABLE OF CONTENT

LIST OF TABLES

LIST OF FIGURES

LIST OF SYMBOLS

Y_c ($p*$)	compressive meridian
$F_{elastic}$	ratio of the elastic strength to failure surface strength
F_{cap} (p)	function that limits the elastic deviatoric stresses
B	the residual failure surface constant
M	residual failure surface exponent
D_1 and D_2	material constants for effective strain to fracture
$G_{fracture}$	shear modulus
$G_{elastic}$	shear modulus
$G_{residual}$	shear modulus
ε_p	effective plastic strain
T_{room}	room temperature
T_{melt}	melting temperature
γ	ratio of specific heat
ρ	air density
E_i	specific internal energy
P	detonation point pressure
$\sigma*$	strength of glass
σ_i*	normalized intact strength
σ_f*	normalized fracture strength
D	damaged scalar

LIST OF ABBREVIATIONS

ALE	Arbitary Langrangian Eulerian
FE	Finite Element
ft	Feet
JWL	Jones-Wilkins-Lee
JC	Johnson and Cook
Kg	Kilogram
lbs	Pound weight
m	Meter
mm	Mili meter
msec	Mili second
MPa	Mega pascal
psi	Pound per Square Inch
RC	Reinforced Concrete
TNT	Trinitrotulene

CHAPTER 1

INTRODUCTION

1.1 Research Background

Blast loading may result from the detonation of high explosive, gas leakage and chemical ammunitions. The force from blast explosion us extremely high, where the force applied over short period of time contrary from normal load. For example, the surfaces of a table and box cannot exert normal forces if both not in contact with each other. Damage to surrounding area such as building damage, collapse and loss life from the epicentre of the explosion cannot be avoided when it occurred. Blast at nearby building are the most reported, either in the war zone or blast due to terrorist attack (Hadden et. al,2007). However, some technic and method for precaution can be used to minimise the impact. Therefore, it is important to understand the blast overpressure behaviour when it next to the building and possible impact from it can be deduce.

The study on the blast effect on structure come to interest due to the attack on the Alfred P.Murrah Federal Building in Oklahama City on 19 April 1995 (Shih-Ho,2016). According to P.Murrah Federal Building the event occur in front of the nine-story because of the truck explosion that set-off by anti-government militant next to the building and about half of the building collapsed (Gumbel,2015). To design building that can fully resist blast load is not realistic and economically. However, with new method and technology, the blast impact on the building or surrounding area can be reduced. One of the effective approach to ensure the safety and reduced the blast impact on the civilian nearby or inside the building is by construct a wall as barrier (Shi,2016).

1.2   Problem Statement

Nowadays explosion event not just occur at war zone, but also reported at civilian area especially at attraction places. This categorised as terrorist attack. The purpose normally to get attention from the authority or want the government fulfil the request. When the explosion occurs at such places, most of the surrounding area including vehicle, building and people are defendless against blast load. The fatal injury and damage on the surrounding are higher in this event. Besides, civilian structure and infrastructure are not design to withstand this kind of load. Therefore, it is necessary to evaluate the blast pressure profile at this situation with and without wall barrier as the protection method. It also necessary to observe blast wave when there is people inside the building. The intensity of this type of load on the building without the wall and wall protection as a barrier need to be assessed. The purpose of this study is to observe the blast profile of buildings with the wall and without wall. Besides that, this study was conducted to know the effect of blast on human inside of the building when there is explosion occur near the building. Other than that, to observe the blast pressure inside and outside of the building when blast happen. In this study, it will focus on the reinforced concrete (RC) wall as barrier at residential area. Numerical analysis will be conducted in three possibility situation which are first with wall, second without next to the building as barrier and the distance of wall with building.

1.3   Objective

The aim of this study was to use RC wall as barrier due to constraint space such as residential area, commercial area and utilities building that developed just next to traffic access such as road, highway and railway station. Hence, the objective of this study are :

- To investigate the blast pressure parameter from 30 lbs. Trinitrotoluene (TNT)

- To study the blast pressure profile on building with wall and without wall as barrier

- To observe the possible effect of blast pressure on human inside the building.

1.4   Scope of Study

In order to achieved the above objective for this research, the scope of this research must be follow as below :

- Numerical modelling of 30 lbs. TNT must be done in ANSYS AUTODYN 3D FE. The experimental result by Yan et. al (2011) will be used to validate the numerical blast pressure of 30 lbs. TNT.

- The numerical analysis would be done on building without RC wall as barrier and building with RC wall as barrier

- The possible impact on human in the building due to blast pressure.

1.5   Significance of Research

This research required to do the simulation in 3-dimensional (3D) numerical model of blast with 13.6 kg (30 lbs. TNT). The blast is modelled and then will be validated by an article reported by Yan et. al (2011) before it can be applied to other parameters. The numerical 3D model is used as reference to the real test.The 3D numerical blast of 30 lbs TNT subjected to building with RC wall and building without RC wall are developed using ANSYS AUTODYN. Therefore, numerical study on blast pressure parameters is possible since civilian researchers had limited access to conduct actual blast test on site. In addition, from the numerical result, further understanding on the possible damaged can be predicted.Besides that, this research is very helpful and beneficial in construction industry since building design in civilian area are not design to withstand the blast. So, this study can be implemented in new invention to developed and construction of the building.Furthermore, this research is very helpful to study on blast load effects and possible damage such as damages on building, infrastructure, injury on human and fatality can be predicted due to the understanding of the pressure parameters numerically and literature review that can provide more information in this research.

1.6   Overview of the Thesis

Chapter 1 presents general view of the research in term of introduction, problem statement, objective, scope of study and significance of research.

Chapter 2, presents the literature review of the study which consists of blast, AUTODYN, blast loading on building and numerical methods.

Chapter 3, presents the flow of methodology of this study to investigate the blast overpressure parameters on the building with and without RC wall numerically.

Chapter 4, it presents the analysis of the result and discussion from the numerical analysis that stimulated in AUTODYN.

Chapter 5, presents the overall summary of the objective of this study and conclusion are presented together with the recommendation for future study.

CHAPTER 2

LITERATURE REVIEW

2.1   Introduction

The number of terrorist attack that has been increase dramatically in few years and decades all many study and investigation had been conducted to know the how the blast pressure travel through out the air. The study was conducted to know the blast profile and how the blast can give impact to human around the world were implemented through bombing and explosion had caused damaged and injured to innocence people. Due to the increasing numbers of the terrorism act that involved with bombing and explosion. In this chapter, it will provide the review from research that related to this study. The previous will be used as guidance and reference in this study that related to the blast that happen near the building.

2.2   Blast

Blast occur when a large amount of energy is released into a small volume of area in a very short time. The energy released when explosion occurs comes in many formed such as chemical (artificial explosives), nuclear and hydrothermal (volcano eruptions).   When explosion occur, the material inside the blast will released concentrated gas that expand quickly to surrounding air space and it also would apply pressure to everything near it. Explosion occur in blink of eyes in very short times (miliseconds) in powerful blast that enough to blow away nearby objects such as buildings, trees and cars. There were three characteristics for explosion which are mechanical, nuclear and chemical (Johnson,2019) .

2.2.1   Types of blast

Mechanical blast depend on physical reaction. For example overloading a container with compressed air. The application was used in device for mining where chemical explosives gas release might be undesirable, but is used very little otherwise. Nuclear explosive can take place almost immediately with a sustained nuclear reaction

and release a large amounts of energy. Nuclear explosives for the potential extraction of petroleum have been tested. Chemical explosions were solid or liquid compound that convert into hot gases. Due to the extremely fast conversion of a solid or liquid compound into hot gases, the chemical explosions are significantly larger than the substances they are produced from. There were two types of chemical explosives which were detonating or high explosives and deflagrating or low explosives. Detonating explosives were high pressure and characterized by extremely quick decomposition, while deflationary explosives such as black and smokeless powders simply involve fast burning and produce relatively low pressure. Example of detonating explosives such as TNT and dynamite. Detonating explosives were divided into two categories :

- Primary explosives detonate by ignition from some source such as flames, sparks, impacts or other means to produce enough heat.

- Secondary explosives Requires a detonator and a additional booster in some cases

Detonation refers to a very rapid and stable chemical reaction. While chemical reaction that proceeds at a speed through the explosive material called the detonation velocity. The range for detonation velocities from 5,000 to 8,000 meters per second for most high explosives. The detonation wave quickly transforms the solid or liquid explosive into a very hot, dense and high-pressure gas. The volume of the explosive gas was the source of powerful air blast waves. The pressure wave for detonation range from 18,000 to 35,000 MPa. The total energy for chemical reaction only available for about one-third when high explosion released in the detonation process. The remaining would be released slowly in air as the detonation products mix with air and burn.

There were various forms of explosives, commonly the explosives called by TNT, PETN, RDX, Semtex and etc. Usually, terrorist often produce their own explosive devices out of ordinary. Usually the product contain material that available in market such as lawn fertiliser and diesel fuel. Those material were easy to get in market because it was legal product until it assembled into a bomb and those materials would behave as high explosive material to ensure that the substantial structures was collapsed or damaged when the bomb was activated. Trinitrotoluene (TNT) was universal in blast resistant design. In order to measures the blast effects from other blast, the actual mass

of the blast need to be converted into TNT equivalent mass by multiplying the mass of explosive by a conversion factor. The energy output ratios of the explosive material were converted to TNT. Table below show the conversion factor for selected explosives.

Table 2.1 Conversion factors for selected explosives.

Explosive	TNT equivalent
TNT (trinitrotoluene)	1.000
RDX (Cyclonite)	1.185
PETN	1.282
Compound B (60% RDX 40% TNT)	1.148
Pentolite 50/50	1.129
Dynamite	1.300
Semtex	1.250

Source : (Remennikov,2007)

2.2.2 Characteristics of the blast wave

Blast wave would cause material damage when there is an explosion near the ground surface due to the shock and accompanies with an explosion. Most of the structures would damage when air blast (overpressure in the blast wave) hit the structures beyond the atmospheric pressure (101 kPa at standard sea level condition) about 3 t0 5 kPa or more. The overpressure level will extend depends on the energy of the explosion and also the distance where the explosion occur.

Gaseous detonation was a high speed load that occurs with a velocity that greater than the velocity of a sound. There were two principal required for detonation to start. First, the formation of a shock wave within an intensity sufficient for an explosive mixture to auto-ignite. Second, an increase in the local rate of energy release to a level sufficient for shock wave reproduction in the adjacent layer in the explosive mixture. A gas wave is formed by a strongly connected shockwave and reaction zone. An ideal gaseous has a velocity that called as Chapman-Jouguet velocity (V_{cj}). The velocity range was about 1500 to 3000 m/s and it depend on fuel-oxidizer combination.

The maximum wave pressured for this load can reached as high as 20 to 30 times the ambient pressure and the gas temperature may exceed 2000 °C (Malekan et. al, 2019).

The hot gases at extremely high pressure can cause shock wave to moving outward at high velocity. This wave was characterized by a very sharp pressure increase on the moving front and a rapid reduction in pressure in the explosion's internal region. At the early stage , the graph show variation of pressure with distance from the centre as shown in Figure 2.1 for an ideal shock. As the blast travels far from the source, the overpressure at the front steadily decreases. After a certain time, when the blast had travel at certain distance, the pressure would drop below atmospheric pressure (negative phase). Overpressure at t_1 to t_5, the blast overpressure is above atmospheric pressure (101 kPa) but when the blast overpressure reach at t_6, at certain distance the blast overpressure reduced below the atmospheric pressure. When this situation happen, the ambient pressure (atmospheric pressure) was called as underpressure rather than overpressure exists. A sudden release of energy when explosion occurs to atmosphere would result a pressure transient or blast wave. The blast wave radiates from the source at supersonic speed in every direction. The magnitude and shape of the explosion wave depend on how much energy was emitted and the distance from the explosion point. Usually high explosives detonation produces a characteristic shape known as an ideal blast wave as shown in Figure 2.2. Shock wave was instantaneous rise in pressure from atmospheric pressure P_o to a peak overpressure P_{so}. The peak overpressure would decreased exponentially to the ambient value in time t_o, which known as positive phase duration. The blast overpressure that below atmospheric pressure (negative pressure) wave with a duration t_n was much longer than the positive phase and characterized as a maximum negative pressure P_n. The negative phase pressure show that, the blast loads acting in the direction that opposite to the original blast wave. Because negative pressure of phases are relatively small and the primary lateral force is different, in a blast-resistant design it is generally conservative to ignore them.
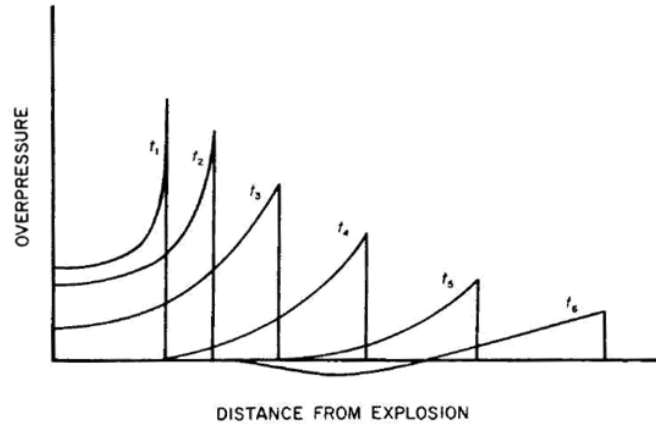
Figure 2.1 Variation of overpressure with distance.

Source: (Remennikov,2007)

As the blast wave propagates through the atmosphere, the air moves outside at lower speed. The velocity of the air particles and wind pressure depends on the peak overpressure of the blast wave. The air velocity is associated with the dynamic (blast wind) pressure, q. Standard relationships have been determined between the peak incident pressure, P_{so}, the peak dynamic pressure, q_o, the wind velocity, and the air density as shown in Figure 2.2
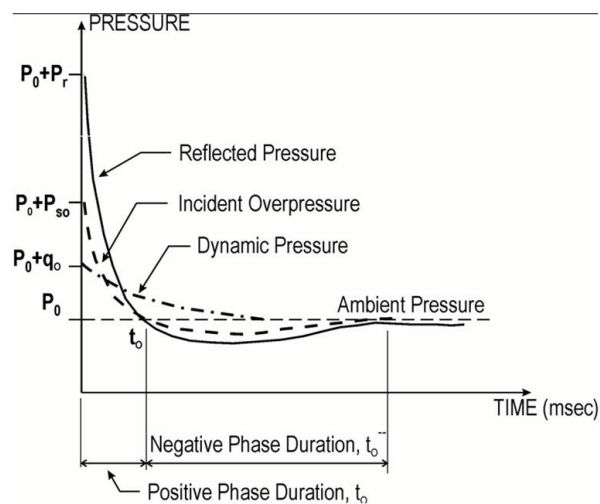
Figure 2.2   Variation of overpressure, dynamic pressure, and reflected pressure with time at a fixed location.

Source: (Remennikov,2007)

2.2.3   Blast Load Classification

Blast loads on structures can be divided into two main groups based on confinement of the explosive charge (unconfined and confined explosions) and it can be subdivided based on the blast loading produced within the structure or acting on structures. The blast loading categories was stated as Table 2.2. Free air blast pressures was an explosion occurs next to and above building structure, initial shock wave will not increase between the explosive charge and the structure. While air burst environment was produced by explosion that occur above the ground surface at certain distance away from the building, to ensure that the initial shock wave propagating away from the explosion and have an impact on the ground surface when it reach the building structure. Besides that, surface burst was the blast environment that located on or near the ground surface. The initial wave of the explosion was reflected and reinforced by the ground surface to produce a reflected wave.

Table 2.2 Blast Load Categories

Charge Confinement	Category	Pressure Loads
Unconfined explosions	1. Free Air Burst	a. Unreflected
	2. Air Burst	b. Reflected
	3. Surface Burst	b. Reflected
Confined explosions	4. Fully Vented	c. Internal shock
		d. Leakage
	5. Partially Confined	c. Internal shock
		e. Internal gas
		d. Leakage
	6. Fully Confined	c. Internal shock
		e. Internal gas

Source: Remennikov (2007)

Blast wave at surface will reflect when the blast wave strikes at a rigid surface such as the ground surface or a front wall. The formation of a reflected surface shown as Figure 2.3. It shows that, there were four stages of the spherical blast waves from air burst. The wave dost not reached ground at the first stage. Wave started to reflect at third stage. The exact value was dependent on the strength of the incident wave and the angle of incidence. The nature of the surface has a major impact too, but is usually considered smooth (or ideal) and therefore it will acts as an ideal reflector. The observed the blast overpressure in time, the point on a surface must not too far from

centre of explosion (as in point A in Figure 2.3). Point A must within the region of "regular" reflection, where the waves reflected and the incident do not merge except on the surface. Two separate blast wave would be recorded . First, the incident due to the blast wave. Second, the blast wave that reflected off the ground that arrived in short times. The situation illustrates such as in Figure 2.3 in point B. At time t_3, the blast wave will reached at this point at certain distance and at time t_4, there were short interval before blast wave reached at point B. The peak for blast overpressure would be less than the value at surface level because the reflected surface has spread out.
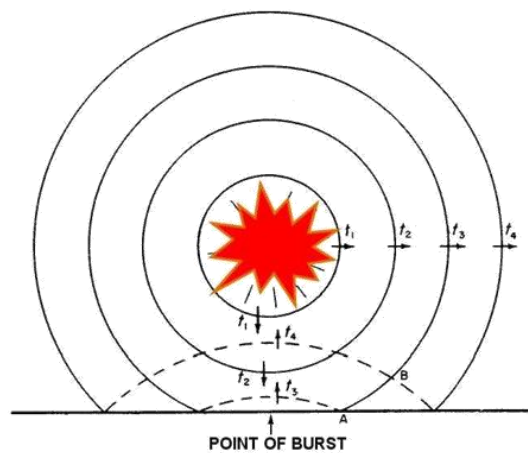
Figure 2.3 Reflection of blast wave at the ground surface for explosion occurring at some distance above ground.
Source: (Remennikov,2007)

Surface explosion differs somewhat from the air explosion. In this type of burst, the incident and reflected shock waves merge instantly (as in Figure 2.4). The shock wave characteristic for an ideal (absolutely rigid) reflecting surface were overpressure and dynamic pressure. At time t_1 to t_4 (as shown in Figure 2.4), there were a single shock front which was in hemispherical form because of the immediate in merging of the incident and reflected blast waves. The shock front was mainly vertical close to the surface, and the dynamic front wind blows horizontally.
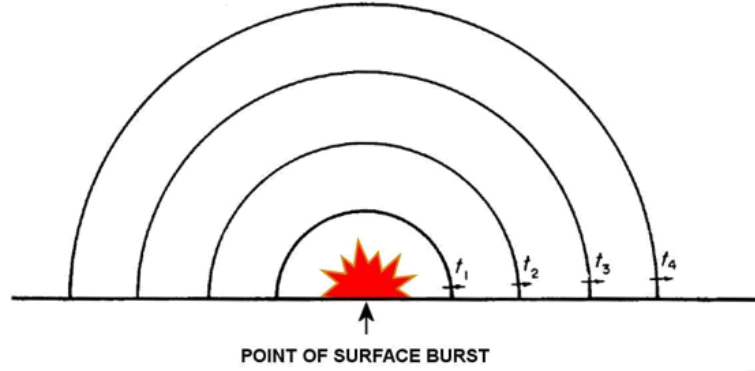
Figure 2.4 Blast wave from a surface burst.

Source: (Remennikov,2007).

2.3   Numerical methods

Numerical methods for explosion and impact can be classified into two categories which were Lagrangian methods and Eulerian methods. Eulerian methods are more suitable to simulate problems with the explosion since Eulerian methods use a fixed mesh to avoid the common problems of the Lagrangian method. Below were the equation for Eulerian.

$$\frac{\partial \rho}{\partial t} + u.\nabla\rho + \rho\nabla.u = 0 \qquad\qquad 2.1$$

$$\frac{\partial u}{\partial t} + u.\nabla u = \frac{1}{\rho}\nabla.\sigma \qquad\qquad 2.2$$

$$\frac{\partial e}{\partial t} + u.\nabla e = \frac{1}{\rho}\nabla.(\sigma.u) \qquad\qquad 2.3$$

where *t, u, ρ* and *e* are the time, *P* and *S* are the hydrostatic pressure and the deviatory pressure which can be obtained from the state equation. σ is the Cauchy stress tensor can be divided into two tensors:

$$\sigma = -PI + S \qquad\qquad 2.4$$

where I is the identity tensor, P and S are the hydrostatic pressure and the deviatory pressure can be obtained from the state equation and the constitutive equations.

Below was gas state equation in the simulation for blasts:

$$P = (k - 1)\rho.e \qquad\qquad 2.5$$

$$k = k_1 + (k_0 - k_1) \exp\left[b\left(\frac{1}{p_0} - \frac{1}{\rho}\right)\right] \qquad\qquad 2.6$$

where P is the pressure, k_0 and k_1 are the polytropic index of detonation products and full expansion detonation products, respectively. b, ρ, ρ_0 are the adjustment coefficient, the local density and the initial density.

2.4   AUTODYN

The AUTODYN software was used to stimulate bon-linear impact phenomena involving large strains ad deformations, plasticity, fracture and flow. AUTODYN will be used to simulate the research because has the capability to solve dynamic problem by using finite elements (FE), finite volume (CFD) and mesh-particle (SPH) to solve nonlinear dynamic problems. AUTODYN 2D and 3D are specifically for fully integrated engineering analysis codes for non-linear dynamic problems. In a single, interactive, graphic menu driven package, AUTODYN includes all required model generation, analysis and display functions. This software were particularly suited for the modelling for impact, penetration, blast and explosion events. AUTODYN-2D and 3D are explicit integration codes, which resolve physical equation of mass, momentum and energy conservation with material descriptions. The available numerical processor in this software were Lagrange (for modelling solid and structures) and Euler (for modelling gases, fluids and solids). AUTODYN also include ALE solver which provide automatic rezoning and applicable to specialized flow problem. While Shell processor for modelling thin structures. Lastly, SPH (Smooth Particle Hydrodynamic) can be used for extreme solid deformations. AUTODYN also include an erosion algorithm that improves the Lagrange processor's ability to simulate problems of impact where major deformations happen. The equations of state include the Linear, Polynomial, Shock, JWL, Ideal Gas, Orthotropic, Porous, Tillotson and PUFF models (Gao,2015). Table below shown the application for AUTODYN.

Table 2.3 Application for AUTODYN

Application	2D	3D	Processors
Hypervelocity Impacts	/	/	Euler, Lagrange and SPH
Ceramic Armor Impact,		/	Lagrange
Oblique Penetration and Ricochet		/	Lagrange
Oil well shaped charge and perforation	/		Euler
Impact and crush of a steel girder		/	Shell

Source: Gao (2015)

Arbitary Lagrange Euler (ALE) was a processor in AUTODYN-2D and AUTODYN-3D were combination for both Lagrange and Euler methods. In Lagrange numerical mesh, the particle motion of the material move with grid points. Lagrange method was useful for solid because material motions do not create large mesh distortion. While in Euler, the numerical mesh stays fixed in space and material would flow through it. Euler was suitable for fluid and gas. It can be applied for solids to but large distortion may occurred. The ALE processor allows the numerical mesh either to move with the material as in a Lagrange mesh, stay fixed in space as in Euler mesh or move in an arbitrarily specified manner to provide continuous and automatic rezoning.

2.4.1 Material Model for Concrete

A correct model that shows concrete material behaviour characteristic at a high stress level is essential in order to achieve a reliable forecast of concrete behaviour under blast loads. The material model for concrete is developed by Riedel, Hiermayer and Thoma (RHT) (Riedel et al., 1999) is adopted. The concrete model includes pressure hardening, third invariant dependence for compressive and tensile meridian. It also can be used for damage model for model strain softening. This model also used by $p - \alpha$ equation of state (Herrman, 1969) that represent concrete for thermodynamic behaviour at high stress, it can reasonably provide description in detailed for the compaction behaviour at low-stress ranges. The specific internal energy for the porous material is estimated to be the same as the solid material at the same pressure and temperature. It consists of three pressure-dependent surfaces, namely, a failure surface

(fracture), an elastic limit surface, and residual strength surface for the crushed material. Figure 2.5 shows these strength surfaces.
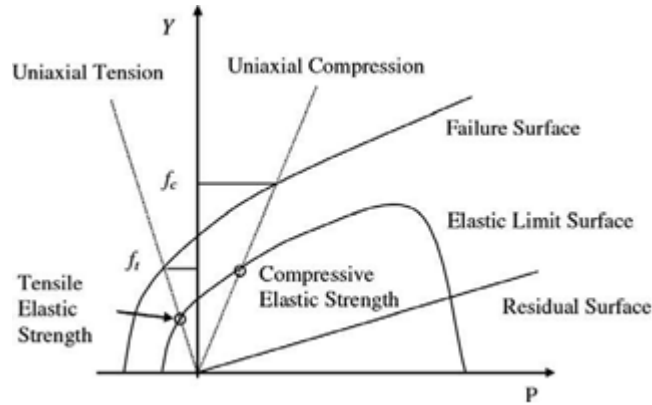
Figure 2.5 Maximum strength, yield strength and residual strength surfaces.

The failure surface, Y_{fail} is defined as a function of the normalised pressure p^*, lode angle θ and strain rate $\dot{\varepsilon}$;

$$Y_{fail}\ (p^*,\theta,\dot{\varepsilon}) = Y_c\ (p^*)\ .\ r_3\ (\theta)\ .\ F_{rate}\ (\dot{\varepsilon}) \qquad\qquad 2.7$$

where $Y_c\ (p^*)$ is the compressive meridian and it is represents by

$$Y_c\ (p^*) = f_c\ [A\ .\ (p^* - p^*_{spall}F_{rate}\ (\dot{\varepsilon}))^N] \qquad\qquad 2.8$$

where, $F_{rate}\ (\dot{\varepsilon})$ represents the dynamic increase factor (DIF) as a function of strain rate $\dot{\varepsilon}$. $r_3\ (\theta)$ defines the third invariant dependence of the model as a function of the second and third stress invariant and a ratio of strength at zero pressure Q_2. Figure below shows the tensile and compressive meridian on the stress π plane.
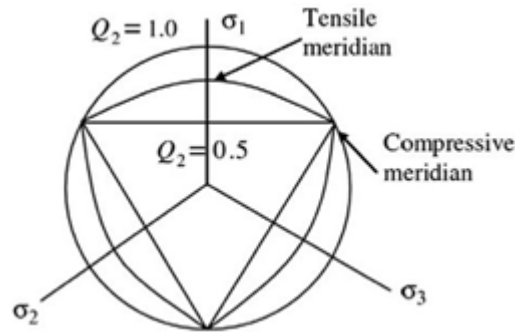
Figure 2.6 Third invariant depend on stress plane.

Source: ANSYS (2011)

The elastic limit surface is scaled from the failure surface,

$$Y_{elastic} = Y_{fail} \cdot F_{elastic} \cdot F_{cap}\ (p)$$ 2.9

where $F_{elastic}$ is the ratio of the elastic strength to failure surface strength. $F_{cap}\ (p)$ is a function that limits the elastic deviatoric stresses under hydrostatic compression, varying within the range of (0,1) for pressure between initial compaction and solid compaction pressure.

The residual failure surface is defined as

$$Y_{residual} = B \cdot (p^*)^M$$ 2.10

where B is the residual failure surface constant and M is residual failure surface exponent.

After hardening phase, additional plastic straining of the material results in damage and strength reduction. Damage is assumed to accumulate using the relationship

$$D = \sum \frac{\Delta\varepsilon_p}{\varepsilon_p^{failure}} = \sum \frac{\Delta\varepsilon_p}{D_1(p*-p*_{spall})^{D_2}}$$ 2.11

where D_1 and D_2 are material constants for effective strain to fracture.

The accumulation can have two effects in the model, reduction in strength and reduction in shear stiffness as below

$$Y^*_{fracture} = (1 - D)\, Y^*_{failure} + DY^*_{residual} \qquad\qquad 2.12$$

$$G_{fracture} = (1 - D)\, G_{elastic} + DG_{residual} \qquad\qquad 2.13$$

where $G_{fracture}$, $G_{elastic}$ and $G_{residual}$ are the shear modulus for the indicated respective parameters.

2.4.2 Material Model for Steel Reinforcement

Johnson-Cook (JC) material model (Johnson & Cook,1983) was used to describe the behaviour of the steel reinforcement. This model represents the strength behaviour of material subjected to large strain, high strain rates and high temperature usually metal. The model defined the yield stress Y as

$$Y = \left[A + B\varepsilon_p^n \right] \left[1 + Cln\frac{\acute{\varepsilon}_p}{\acute{\varepsilon}_0} \right] \left[1 - T_H^m \right] \qquad\qquad 2.14$$

where ε_p is effective plastic strain; $\acute{\varepsilon}_p = \frac{\acute{\varepsilon}_p}{\acute{\varepsilon}_0}$ is normalised effective plastic strain rate for $\acute{\varepsilon}_0 = 1s^{-1}$; homologous temperature, $T_H = (T - T_{room}) / (T_{melt} - T_{room})$ where T_{room} is room temperature T_{melt} is melting temperature and A, B, C, n and m are five material constants. First, second and third bracket in the equation represents the stress as a function of strain, effect od strain rate on the yield strength and thermal softening, respectively. Constant A as basic yield stress at low strain. While B and n represent the effect of strain hardening.

2.4.3 Material Model for Air and High Explosive

The numerical approach for the interface analysis between air and structure is the Arbitary Lagrange Euler (ALE). Different parts of the solvers such as structure, fluids and gases can be modelled simultaneously by using Lagrange and Euler approaches. This different solver will be coupled in space and time.

Air is modelled by an ideal gas EOS in numerical model. The pressure is related to energy and is given by

$$p = (\gamma - 1) \rho E_i \qquad\qquad 2.15$$

where γ is a ratio of specific heat and ρ is air density, E_i is the specific internal energy. The standard constant of air in AUTODYN are air density $\rho = 1.255$ kg/m^3, $\gamma = 1.4$ and air initial internal energy, $E_i = 2.068 \times 10^5$ kJ/kg.

TNT known as high typically modelled by using the Jones-Wilkins-Lee (JWL) EOS, which model the pressure generated by chemical energy and can be represented as follows

$$P = A \left(1 - \frac{\omega}{R_1}\right) e^{-R_1 V} + B \left(1 - \frac{\omega}{R_2 V}\right) e^{-R_2 V} + \frac{\omega E_i}{V} \qquad\qquad 2.16$$

where P is the detonation point pressure of high explosive; V is the specific volume; E_i is the specific internal energy; and A, B, R_1 and ω are material constant which have been determined from dynamic experiments.

2.4.4 Material Model for Glass and Wood

Glass is one of the material model used for structures in building. The major reason for special care in the design of glass is that it has no ductility to allow a moment or force redistribution like steel and concrete frames. In general, glass is known as structure with smaller in thickness than its lateral dimensions. Its can resist the external forces by the combination of membrane and bending actions. The bending and membrane stiffness must be considered in analysis to model the structures with such behaviour. A two-dimensional mathematical model, Kirchhoff Thin Shell Theory of Plates, determines stresses and deformations in thin plates subject to forces and moments.

The glass model was modelled with Johnson Holmquist Strength Continuous model (Yusof et. al, 2014). This material model was developed by Holmquist in 1995 and hence namely as JHS model. This model described standard material model of float glass in AUTODYN material library. JHS model has considered both the strain rate effect and the material damage. Glass is known as brittle type of failure and it assumed to occur when the maximum stress attains the fracture tensile strength of glass. The

failure and breakage of glass is, generally speaking, due to the stress concentrated at the invisible hairy cracks on its surface. The failure stress of a piece of glass is more dependent on the density of these hairy cracks than on the theoretical breakage stress which can be as high as 14000 MPa (Kwok et. al,1996).

$$\sigma^* = \sigma_i^* - D(\sigma_i^* - \sigma_f^*) \qquad\qquad 2.17$$

where σ^* is the strength of glass, σ_i^* is normalized intact strength, σ_f^* is normalized fracture strength and D is damaged scalar.

Wood is one of the material model used for structures in building. Wood may be described as an orthotropic material; that is, it has unique and independent mechanical properties in the directions of three mutually perpendicular axes which are longitudinal, radial, and tangential. The longitudinal axis L is parallel to the fiber (grain); the radial axis R is normal to the growth rings (perpendicular to the grain in the radial direction); and the tangential axis T is perpendicular to the grain but tangent to the growth rings.

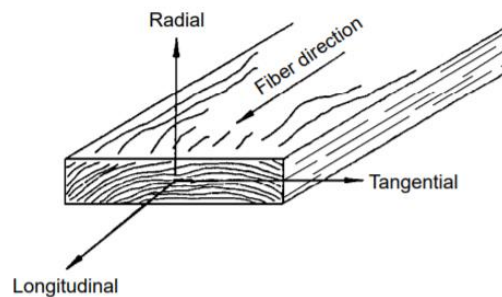Figure 2.7 Three principles axes of wood with respect to grain direction and growth rings.

Source: Green et. al (1999)

The modulus of elasticity and Poisson's ratios are used to calculated elastic properties of the wood behaviour. The modulus of elasticity and Poisson's ratios are related by expressions of the form

$$\frac{\mu_{ij}}{E_i} = \frac{\mu_{ji}}{E_j} =, i \neq j \ \ i,j = L,R,T \qquad\qquad 2.18$$

where E is modulus of elasticity; µ is Poisson's ratio and; L,R and T is longitudinal axis, radial axis and tangential axis.

2.5   Blast effect

Design of building that resist to blast load had been implemented since incident 11 September. There were many study had been conducted about how building can resist blast load especially area that was not in war zone. 10 story building with reinforced concrete (RC) had been study (Danesh,2017). The building was subjected with hemispherical blast with 1000 kg TNT. It was located at different standoff distance. The study was conducted to make comparison of response of building structures to blast load and seismic excitations. From the study it shows that blast loads had much higher force to the structures than seismic action that cause the structures to deforms more. When there attack on public facilities such as shopping malls, metro stations and etc it would result in serious threat on people's lives and property. When the explosion blast wave acts on human body it would leads to injury, damage internal organ, trauma, fracture or died. But when the blast wave acts on building it would cause the building to collapse and damage. The blast at peak pressure was much higher when the blast act on structures than in the free field explosion because the blast wave on structures more higher that can cause the damage to the entire structures and it can lead to the overall collapse. The human and buildings vulnerability under the explosive blast loading (Ma et. al,2017) and Effect of various long duration blast overpressures and the associated maximum wind speed on various structures and the human body (Zipf et. al,2010) was shown in below.

Table 2.4 The human and buildings vulnerability under the explosive blast loading.

	Damage degree	Shockwave pressure (10^5 Pa)
Human	Mild contusion	0.2 – 0.3
	Medium damage (Auditory organ damage and fracture etc.)	0.3 – 0.5
	Serious injury (internal organs damage which may lead to death)	0.5 – 1.0
	Very serious injury (most lead to death)	>1.0
Buildings	Door and window damage	0.05 – 0.15
	Window frame damage	0.15 – 0.2
	Wall cracks	0.2 – 0.3
	Wall cracks, roofing tile fell off	0.4 – 0.5
	Wooden building workshop pillar broken	0.6 – 0.7
	Brick wall collapsed	0.7 – 1.0
	Small houses collapsed	1.0 – 2.0
	Large steel frame structure damage	2.0 – 3.0

Source : Ma (2017)

Table 2.5 Effect of various long duration blast overpressures and the associated maximum wind speed on various structures and the human body.

Pressure	Max Wind speed	Effect on structures	Effect on the human body
1 psi	38 mph	Window glass shatters	Light injuries from fragments occur
2 psi	70 mph	Moderate damage to houses (windows and doors blown out and severe damage to roofs)	People injured by flying glass and debris
3 psi	102 mph	Residential structures collapse	Serious injuries are common, fatalities may occur
5 psi	163 mph	Most buildings collapse	Injuries are universal, fatalities are widespread
10 psi	294 mph	Reinforced concrete buildings are severely damaged or demolished	Most people are killed
20 psi	502 mph	Heavily built concrete buildings are severely damaged or demolished	Fatalities approach 100%

Source: Zipf et. al (2010)

2.6   Summary

In this chapter, several experiments and numerical methods had been discussed. Most of the studies was focused on blast on structures in order to validate the design and distance standoff that suitable for the building to be constructed. In this chapter, it also discussed about the possible condition of people inside of the building when explosion occurred. Normally building that build not in war zone and located at commercial are usually design not to withstand blast. Because of this, when there was explosion occurred the building would damage or become entirely collapsed. If there was human inside the building, the people inside either would only have light injury, fracture or died. For the numerical simulation, software such as AUTODYN and LS-DYNA have been used to validated the behaviour of the building using Lagrange and Euler as their processor.

CHAPTER 3

METHODOLOGY

3.1   Introduction

In this chapter, methodology work of the process would be describes on how the simulation would be done. The simulation would be conducted in 3 cases and all the cases would be simulated in AUTODYN 3D non-linear FE software. The first case, blast with 30 lbs TNT would be simulated at open space. For the second case, the blast with 30 lbs TNT would be simulated on the building without the presence of RC wall. For the third case, 30 lbs TNT would be simulated on the building with the presence of RC wall as barrier. Below figure showed the overall methodology that would presence in this study:
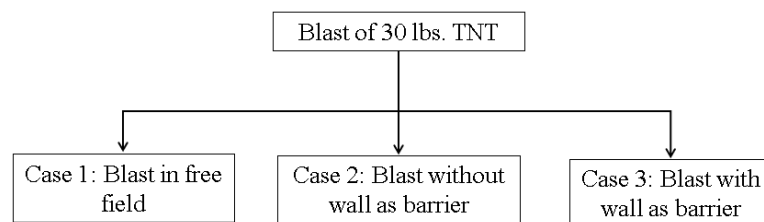

Figure 3.1 Flowchart for the methodology

3.2   Numerical Modelling in AUTODYN 3D RC Wall and Building Subjected to Blast Load

AUTODYN was used for the numerical analysis in this study. AUTODYN was selected to use in this study because it had Lagrangian and Eulerian method. Both Lagrangian and Eulerian were suitable to use to stimulate for solid structure and ideal gas. The ALE (Arbitary Lagrange Euler) solver was used as mesh-base hybrid between Lagrangian and Eulerian method as shown in figure below.
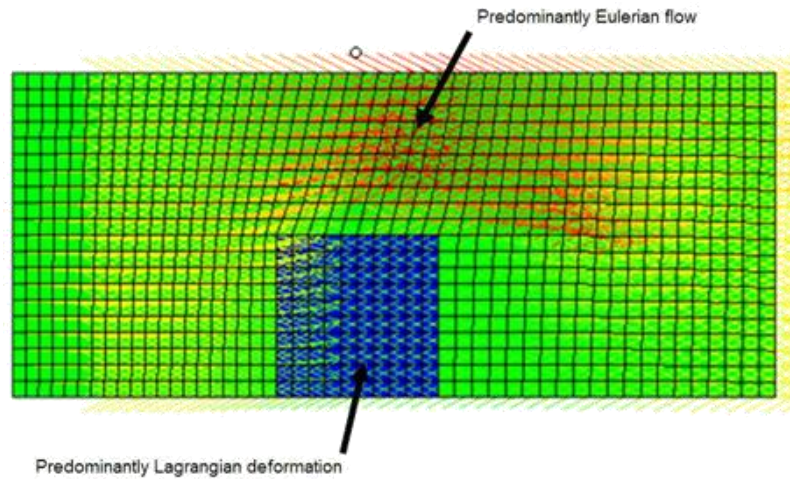
Figure 3.2 ALE solver technique in AUTODYN.

Source: ANSYS (2011)

Before RC wall and building can be imported into AUTODYN solver the analyse the blast overpressure, the both structure need to be identify as solid element to be performed in ANSYS- Workbench. In the analysis, the line body is used for the steel reinforcement in concrete and treated as a perfect link between stainless steel reinforcement and concrete. The eight nodes hexahedral element as shown in Figure 3.3 is used for solid element. The element suited to the transient dynamic applications including large deformations, large strains, large rotations and complex contact conditions. The element formulation based upon the work of Wilkins et al., (1974) results in an exact volume calculation even for distorted elements.
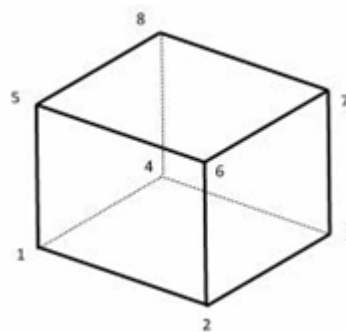

Figure 3.3 Eight nodes hexahedral element.

Source: ANSYS (2011)

Figure 3.4 illustrate the detail for RC wall in this study. The reinforcement for vertical is 16 mm diameter and the horizontal is 10 mm diameter with 152 mm spacing. The concrete covers that covers all sides of the wall with thick 25 mm. The cylinder compressive strength of the concrete is 44 MPa with a standard deviation of 1.38 MPa

whilst the Modulus of Elasticity is 31.5 GPa with a standard deviation of 827 MPa. The reinforcement has a yield strength of 619 MPa and a Young's modulus of 200 GPa. The walls have a cross-sectional dimension of 1 829 mm u 1 219 mm with the wall thickness of 152 mm and 305 mm thickness of footing. Figure 3.5 shows the RC wall meshed with the coarse hexahedral element.
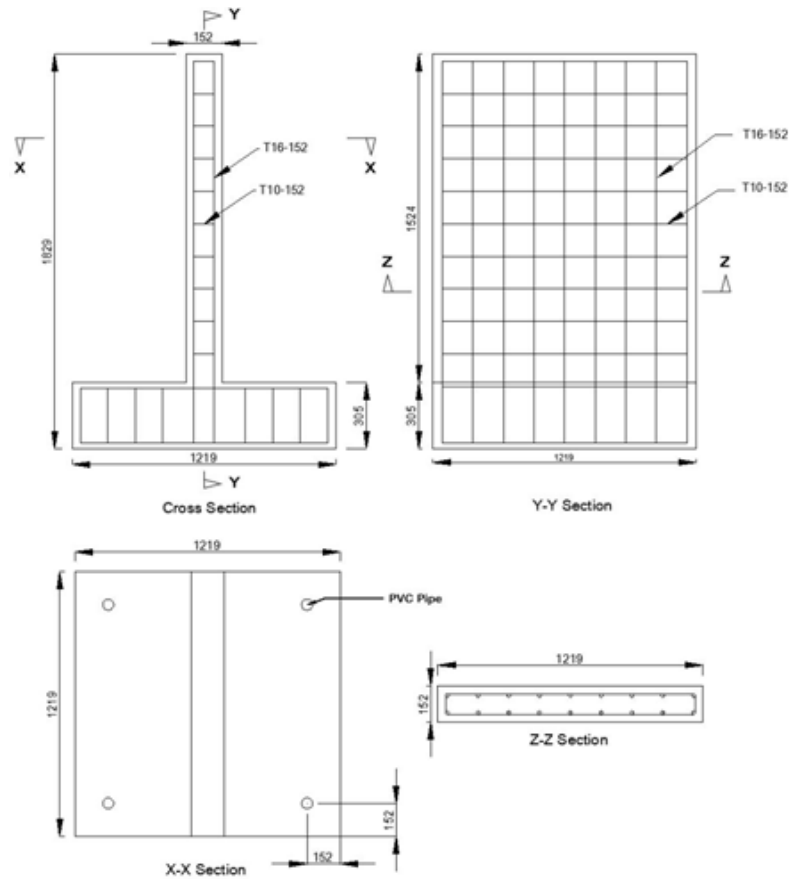
Figure 3.4 Detail of RC wall (Unit: mm).
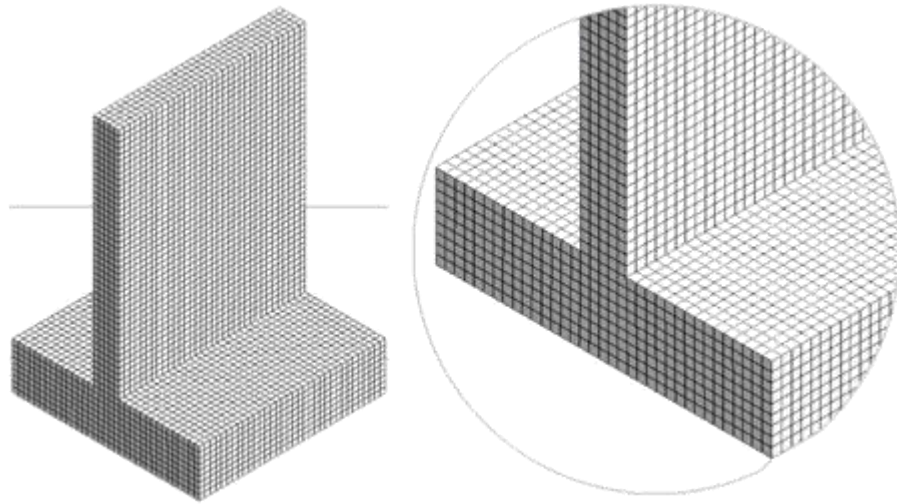Source: Chen et al. (2008) and Yan et al. (2011)

Figure 3.5 Hexahedra meshing of RC wall.

The material model for CONC-35MPA was describe behaviour of concrete in the AUTODYN material library as in Table 3.1. This material was developed by Riedel, Hiermayer and Thoma (RHT) (Riedel, Thoma & Hiermayer,1999). Besides that, to describe the behaviour of the steel reinforcement the standard model of STEEL-4340 in the AUTODYN library is used. This material model was developed by Johnson and Cook (JC) (Johnson and Cook, 1983) and is known as the JC model.

Table 3.1 Input data of STEEL-4340, JC model

Equation of state	Linear	
Reference density	7.83E+00	(g/cm^3)
Bulk modulus	1.59E+08	(kPa)
Reference temperature	2.95E+02	(K)
Specific heat	4.77E+00	(J/kg K)
Thermal conductivity	0.00E+00	(J/mKs)
Strength	Johnson Cook (JC)	
Shear modulus	8.18E+07	(kPa)
Yield stress	7.92E+05	(kPa)
Hardening constant	5.10E+05	(kPa)
Hardening exponent	2.36E-01	(none)
Thermal softening exponent, m	1.03E+00	(none)
Melting temperature	1.79E+03	(none)
Ref. strain-rate (1/s)	1.00E+00	(none)
Failure	None	
Erosion	None	

Figure 3.6 illustrates the detail for building. The length of the building is 6094 mm, the width is 2438.4 mm and the height is 2590 mm. Figure 3.7 shows the building meshed with the coarse hexahedral element.
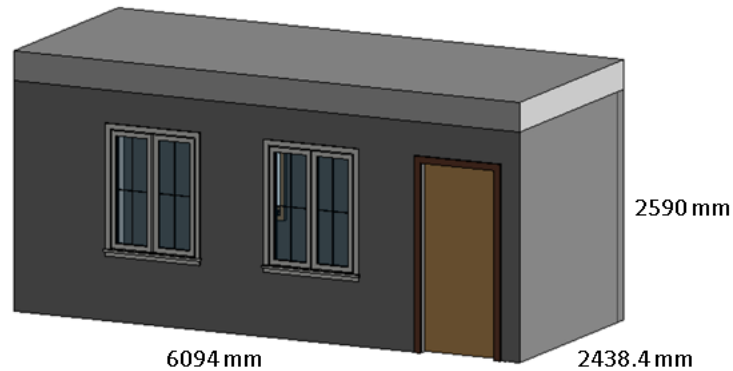

2590 mm

6094 mm   2438.4 mm

Figure 3.6 Dimension for the building.
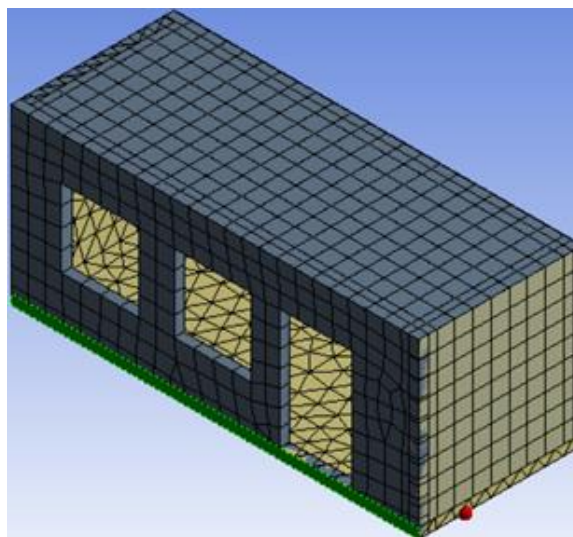
Figure 3.7 Hexahedra meshing for building.

For building, the standard material model for CONC-35MPA was describe behaviour of concrete in the AUTODYN material library as in Table 3.1. This material was developed by Riedel, Hiermayer and Thoma (RHT) (Riedel, Thoma & Hiermayer,1999). Besides that, to describe the behaviour of the steel reinforcement the standard model of STEEL-4340 in the AUTODYN library is used. This material model was developed by Johnson and Cook (JC) (Johnson and Cook, 1983) and is known as the JC model. While the other material used for the building are zinc for roof, glass for window and wood for door.

Table 3.2 Input data of CONC-35MPA material model in AUTODYN

Equation of state	Value	
Density, ρ	2314.00E+00	(kg m-3)
Specific Heat, Cρ	654.00E+00	(J kg-1 C-1)
RHT Concrete Strength	**Value**	
Compressive Strength, fc	3.50E+07	(Pa)
Tensile Strength, ft/fc	0.10E+00	(none)
Shear Strength, fs/fc	0.18E+00	(none)
Intact Failure Surface Constant A	1.60E+00	(none)
Intact Failure Surface Exponent, n	0.61E+00	(none)
Tension/Compression Meridian Ratio Q2.0	0.68E+00	(none)
Hardening Slope	2.00E+00	(none)
Elastic Strength /ft	0.70E+00	(none)
Elastic Strength / fc	0.53E+00	(none)
Fracture Strength Constant B	1.60E+00	(none)
Fracture Strength Exponent, m	0.61E+00	(none)
Compressive Strain Rate Exponent, α	0.032 E+00	(none)
Tensile Strain Rate Exponent, δ	0.04 E+00	(none)
Maximum Fracture Strength Ratio SFMAX	1.00E+20	(none)
Damage Constant, D1	0.04 E+00	(none)
Damage Constant, D2	1.00 E+00	(none)
Minimum Strain to Failure	0.01 E+00	(none)
Residual Shear Modulus Fraction	0.13 E+00	(none)
Bulk Modulus	3.527E+10	(Pa)
Shear Modulus	1.67E+10	(Pa)
Polynomial EOS	**Value**	
Parameter A1	3.527E+10	(Pa)
Parameter A2	3.958E+10	(Pa)
Parameter A3	9.04E+09	(Pa)
Parameter B0	1.22 E+00	(none)
Parameter B1	1.22 E+00	(none)
Parameter T1	3.527E+10	(Pa)
P-alpha EOS	**Value**	
Solid Density	2750.00E+00	(kg m-3)
Porous Soundspeed	2920.00E+00	(ms-[1])
Initial Compaction Pressure, Pe	2.33E+07	(Pa)
Solid Compaction Pressure, Ps	6.00E+09	(none)
Compaction Exponent, n	3.00 E+00	(none)
Failure	**Value**	
Maximum Tensile Stress	1.00E+20	(Pa)
Maximum Shear Stress	1.00E+20	(Pa)
Erosion	**None**	

Table 3.3 Input data of STEEL 4340 material model in AUTODYN

STEEL 4340	Value	
Density	7830.00E+00	(kg m^{-3})
Specific Heat, Cρ	477.00E+00	(J kg^{-1} C^{-1})
Johnson Cook Strength	**Value**	
Initial Yield Stress	7.90E+08	(Pa)
Hardening Constant	5.10E+08	(Pa)
Hardening Exponent	0.26 E+00	(none)
Strain Rate Constant	0.014 E+00	(none)
Thermal Softening Exponent	1.03 E+00	(none)
Melting Temperature	1519.90E+00	(^{0}C)
Ideal Gas (EOS)	**Value**	
Reference Temperature	293.00 E+00	(K)
Bulk Modulus	1.59E+10	(Pa)
Shear Modulus	8.18E+10	(Pa)
Failure	**Value**	
Maximum Tensile Stress	1.00E+20	(Pa)
Maximum Shear Stress	1.00E+20	(Pa)
Maximum Principal Strain	1.00E+20	(none)
Maximum Shear Strain	1.00E+20	(none)
Erosion	**None**	

Table 3.4 Input data of Wood material model in AUTODYN

Wood	Value	
Density	700.00E+00	(kg m^{-3})
Specific Heat, Cρ	2310.00E+00	(J kg^{-1} K^{-1})
Vaporization Temperature	400.00E+00	(K)
Boiling Point	400.00E+00	(K)
Binary Diffusivity	4.00E-05	(none)
Volatile Fraction	0.80 E+00	(none)
Combustible Fraction	0.20 E+00	(none)
Scattering Factor	0.90 E+00	(none)
Burn Stoichiometry	2.67 E+00	(none)
Burn Hreact	3.2789E+07	(none)
Burn Hreact Fraction	0.30 E+00	(none)
Devolatilization Model	20.00 E+00	(none)
Swelling Coefficient	1.00 E+00	(none)
Emmissivity	0.90 E+00	(none)

Table 3.5 Input data of Glass material model in AUTODYN

Glass	Value	
Density	2500.00E+00	(kg m^{-3})
Isotropic Thermal Conductivity	1.40E+00	(W m^{-1}C^{-1})
Specific Heat, Cρ	750.00E+00	(J kg^{-1} C^{-1})

Table 3.6 Input data of Zinc material model in AUTODYN

Zinc	Value	
Density	7140.00E+00	(kg m^{-3})
Isotropic Thermal Conductivity	115.50E+00	(W m^{-1}C^{-1})
Specific Heat, Cρ	389.00E+00	(J kg^{-1} C^{-1})

3.3   Numerical Modelling for blast load 13.6 kg (30 lbs.) TNT

In AUTODYN, the initial detonation for the explosive and blast wave propagation were modelled with an axially symmetric wedge shape. The blast wedge would filled with 150 mm of 30 lbs TNT radius inside 1000 mm radius of air at the outside of the remaining region. The blast wedge was modelled as Figure 3.8 below.
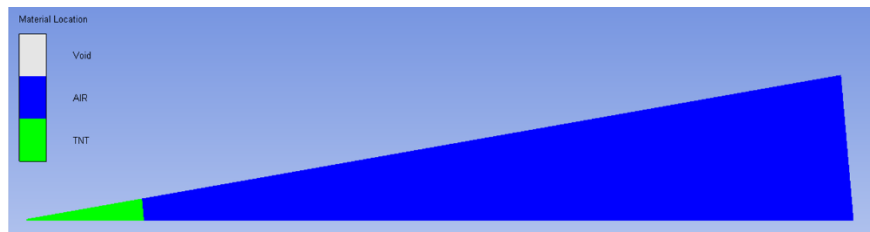

Figure 3.8 The 1m wedge (2D) filled with 30 lbs TNT and air

The detonation would be initiate and run until the blast wave reached 1m from the centre of detonation as shown in Figure 3.9. The blast pressure history would be documented and would be mapping into 3D air volume. The air volume   in the AUTODYN used to describe the behaviour of the air through the ideal gas equation of state (EOS).
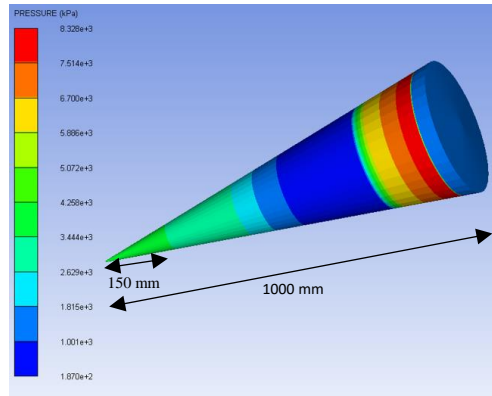
Figure 3.9 Pressure Contours in 1 m wedge (3D) during solving progress

The standard constant air in AUTODYN library for material is used to describe behaviour of the air as the ideal gas equation of state (EOS). While standard model of TNT behaviour would be described by Jones-Wilkins-Lee EOS where the parameters from Dobratz and Crawford (1985) were implemented. Properties for the material were listed at Table 3.7 and Table 3.8.

Table 3.7 Employed material data for air, input to the ideal gas EOS

Equation of state	Ideal Gas	
Reference density	1.22500E+00	(kg m^3)
Specific Heat	7.17600E+02	(J kg^{-1} C^{-1})
Adiabatic exponent, Υ	1.40000E+00	(none)
Reference temperature	1.50500E+05	(C)
Specific internal energy	2.00000E+05	(J kg^{-1})

Table 3.8 Employed material data for TNT, input to the JWL EOS

Equation of State	JWL	
Reference density	1.63000E+00	(g cm^{-3})
Parameter A	3.73770E+08	(kPa)
Parameter B	3.74710E+06	(kPa)
Parameter R_1	4.15000E+00	(none)
Parameter R_2	9.00000E-01	(none)
Parameter ω	3.50000E-01	(none)
C-J Detonation velocity	6.93000E+03	(ms^{-1})
C-J Energy / unit volume	6.00000E+00	(kJ m^{-3})
Strength	**None**	
Failure	**None**	
Erosion	**None**	

3.4   Blast Pressure Analysis

The air volume Type 1 was initially used to asses blast pressure of the calculated explosive (30 lbs TNT) in free field with certain standoff distance from the detonation point. The peak blast pressure in free field will be compared with the reference article (Yan et. al, 2011) to validate the result from numerical analysis in AUTODYN. Below table shown the detail for air volume type.

Table 3.9 Detail of air volume types

Air Volume Type	Air Volume Size in (I,J,K) direction	Volume (m^3)
Type 1	13.4 m x 4.2 m x 14.5 m	816.06
Type 2	13.4 m x 4.2 m x 14.5 m	816.06
Type 3	13.4 m x 4.2 m x 14.5 m	816.06

3.4.1   Air Volume Type 1

Figure 3.11 shows the 3D model and the blast pressure vectors in air volume Type 1 with number of segment of I,J,K (18,22,72). The pressure gauge was placed at the standoff distance 18 feet from detonation point. Flow-out of the air was along the air volume border.
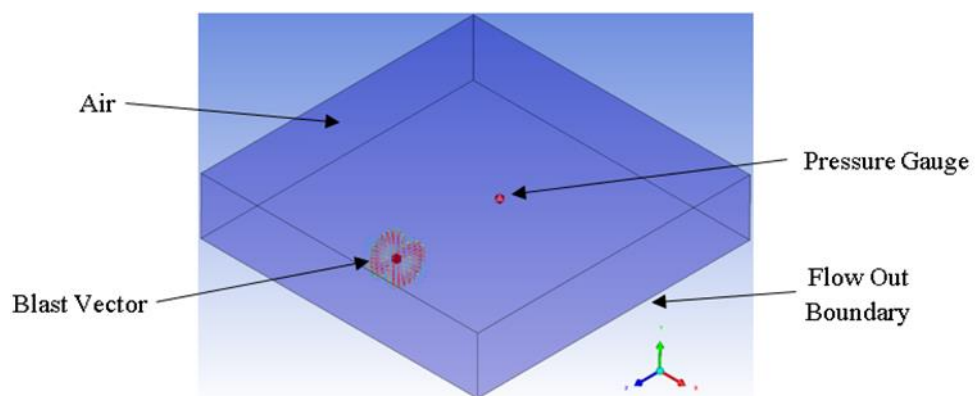

Figure 3.10 Blast simulation in free field (Air Volume Type 1)

3.4.2 Air Volume Type 2

Figure 3.12 show shows the 3D model and the blast pressure vectors in air volume Type 2 with number of segment of I,J,K (18,22,72). The building was placed at the distance about 4500 mm from the detonation point. The pressure gauge was placed along the distance and also inside the house.
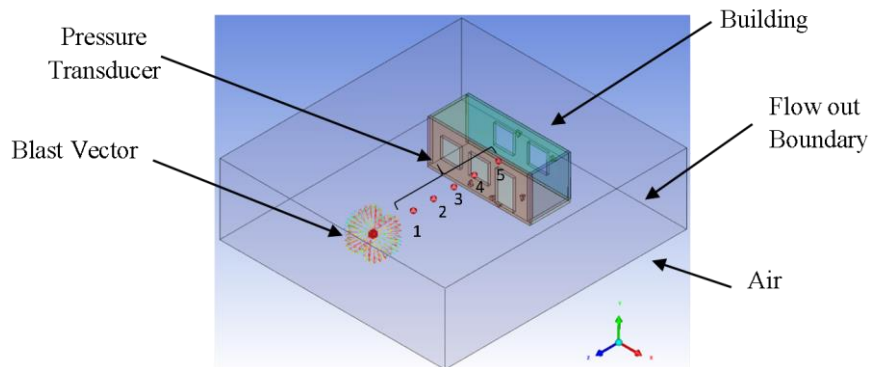

Figure 3.11 Blast simulation without wall (Air Volume Type 2)

3.4.3 Air Volume Type 3

Figure 3.13 show shows the 3D model and the blast pressure vectors in air volume Type 2 with number of segment of I,J,K (18,22,72). The building was placed at the distance about 4500 mm from the detonation point. The pressure gauge was placed along the distance and also inside the house. The RC wall was placed at standoff distance from the detonation point at 1219 mm (4ft.).
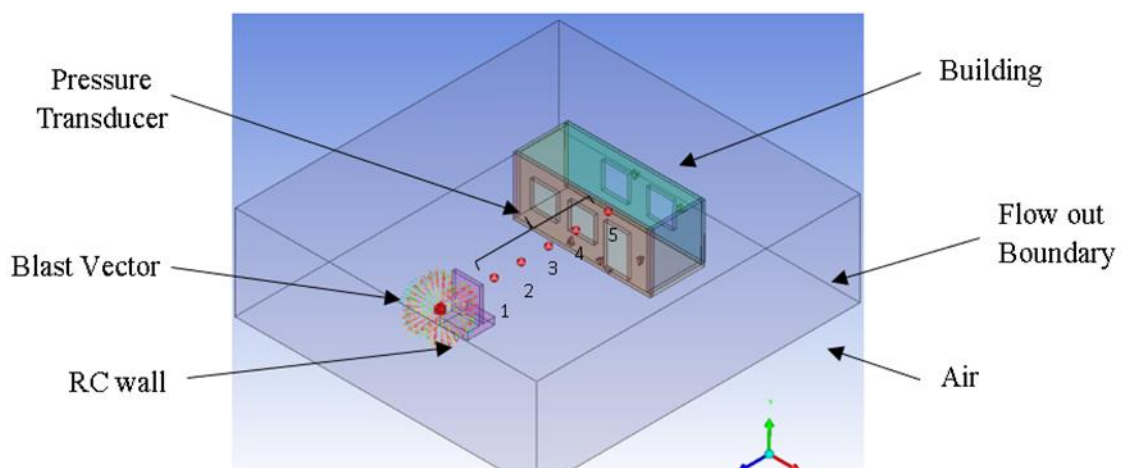

Figure 3.12 Blast simulation with wall (Air Volume Type 3)

3.5   Summary

This chapter represent the flow of methodology of this current study. The numerical blast pressure (30 lbs TNT) would be assigned in three types air volume. Initially the blast wedge will be run in the AUTODYN and it would be documented before it can be remapped into air volume. The blast pressure (30 lbs TNT) would be stimulated in free field (air volume Type 1) and the peak pressure would be validated by the article reference (Yan et. al, 2011) before it can be used by other parameters (air volume Type 2 and Type 3). The present numerical work was carried out in AUTOFYN. Lagrangian solver was used to mesh solid for RC wall and building. While Eulerian solver would be used for the air. Both solver was combined in ALE to solve the blast pressure in AUTODYN.

CHAPTER 4

RESULT AND DISCUSSION

4.1   Introduction

This chapter represent the analysis of the result of blast pressure parameter on building. This analysis consists of three cases that need to be analyse. The first case was focused on blast pressure at free field with the standoff distance 5.486 m (18 ft.) from detonation point. The blast pressure parameter for this case will be validated with related study done by Yan et. a1 (2011). The second and third cases would be stimulated on building using the same blast pressure (30 lbs TNT). For numerical modelling, three type of air volume was assigned to simulated the blast pressure parameter on building. Different parameters were assigned in this study to observe and understand more about the movement of blast wave parameter.

4.2   Blast Pressure Analysis in AUTODYN

The blast pressure parameter will be discussed in this following section by simulated blast pressure of 30 lbs TNT in AUTODYN for various type of air volume.

4.2.1   Air Volume Type 1

The result from AUTODYN show that, the peak blast pressure parameter at distance 5.486 m (18 ft.) as Figure 4.1 was 494.4 kPa at 4.62 msec. Figure 4.1 also shows the peak blast pressure parameter reported by Yan et. al (2011) was 494.4 kPa at 4.64 msec. The blast (30 lbs TNT) use in this study was close to the peak blast pressure test reported by Yan et. al (2011) but the duration for the blast pressure simulated for free field at peak pressure was found to be a little bit shorter at 4.62 msec than the blast test reported (Yan et. al,2011) at 4.64 msec. From the comparison, it shows that the blast (30 lbs TNT) was valid to use for other parameter because the peak pressure between simulation and blast test (Yan et. al,2011) was similar. Figure 4.2 shows blast vectors propagation at free field.
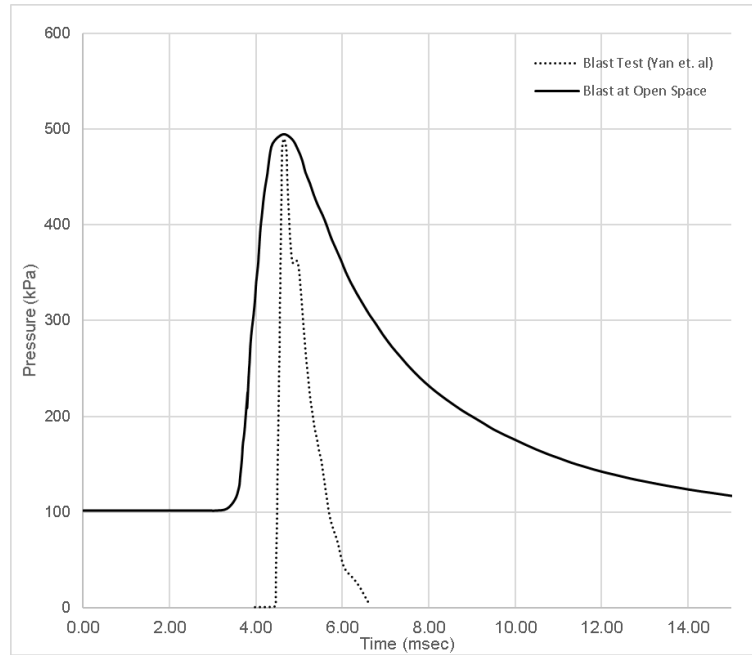
Figure 4.1 Comparison of blast pressure at free field and Yan et. al (2011)
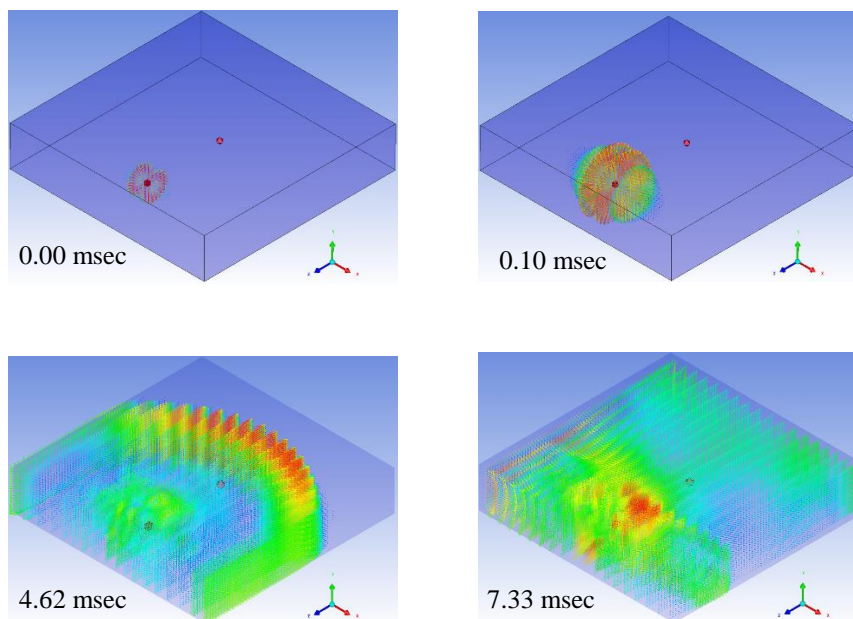

Figure 4.2 Blast wave propagation at free field reach 5.486 m

4.2.2 Air Volume Type 2

Figure 4.3 and Figure 4.4 shows the blast pressure parameter at the distance 4.500 m and 7.050 m from the detonation point without RC wall as barrier. In Figure 4.3, the result from simulation shows the blast pressure result at the distance 1.219 m, 2.438 m, 3.657 m and 4.500 m with the peak blast pressure 1255.63 kPa at 0.22 msec,

458.30 kpa at 1.32 msec, 264.36 kPa at 2.97 msec and 233.26 kPa at 4.09 msec. While in Figure 4.4, the results from simulation shows the blast pressure at the distance 6.050 m and 7.050 m with the peak blast pressure 156.37 kPa at 6.81 msec and 122. 35 kPa at 11.37 msec. According to the figure, it shows that the peak blast pressure at distance 1.219 m recorded the highest blast pressure 1255.63 kPa at 0.22 msec followed by blast pressure at distance 2.438 m, 3.657 m and 4.500 m. The blast pressure recorded inside the building reduce at the distance 6.050 m of 156.37 kPa at 6.81 msec away from the detonation point. Figure 4.5 show the blast vectors propagation. At 0 msec, the pressure is at 101 kPa in atmospheric pressure. At 0.07 msec, the blast wave start to move. At 5.73 msec, the figure show that the blast vector start to hit the building. At 11.37 msec, the blast wave occupied the air domain.
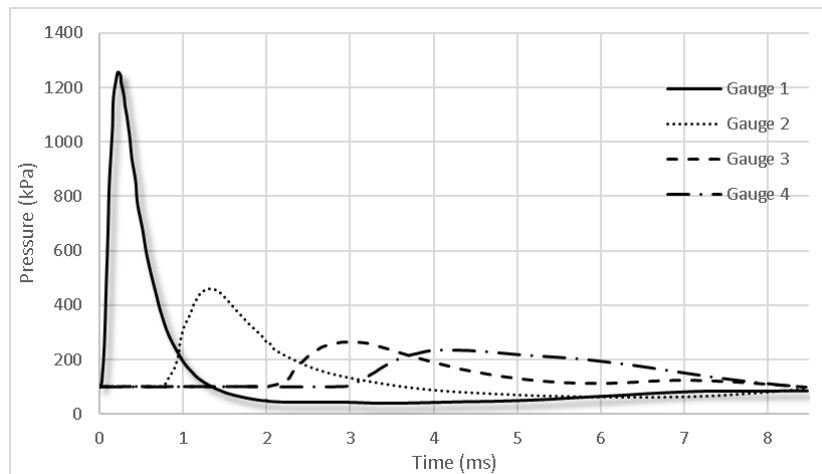

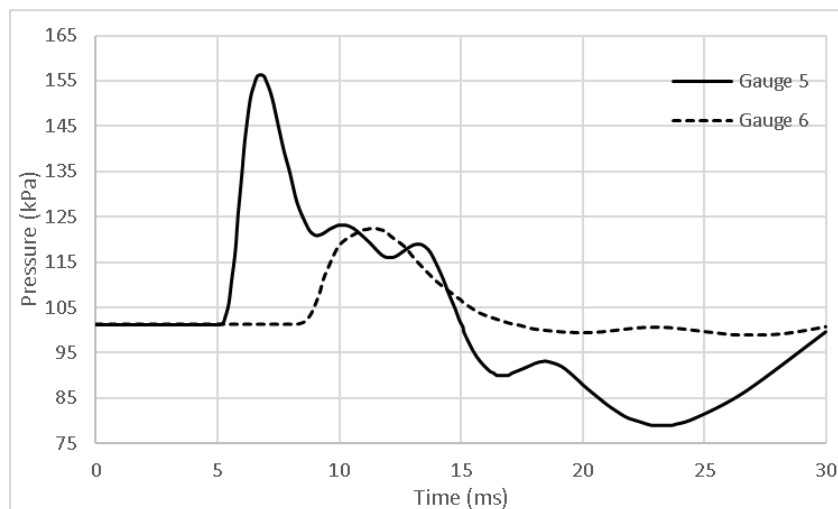Figure 4.3 Blast pressure parameter without RC wall

Figure 4.4 Blast pressure parameter inside and outside of the building without RC wall.
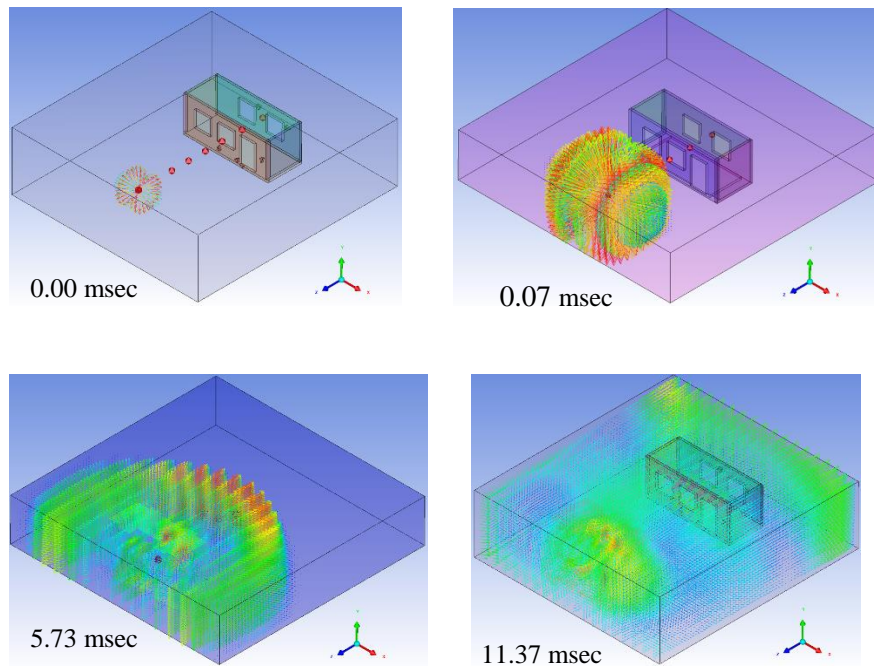
Figure 4.5 Blast wave propagation without RC wall

4.2.3 Air Volume Type 3

Figure 4.6 and Figure 4.7 shows the result of blast pressure parameter with RC wall as barrier. From Figure 4.6 it shows that the peak blast pressure parameter at distance 1.219 m was 315.24 kPa at 1.66 msec recorded as the highest blast pressure. The peak blast pressure reduce as the distance increase. At distance 2.438 m, 3.657 m and 4.500 m, the blast pressure record the peak blast pressure of 236.61 kPa at 3.65, 191.45 kPa at 5.89 and 170.43 kPa at 8.86 msec. For Figure 4.7 it shows the result of blast pressure inside and outside of the building with RC wall as barrier at distance 6.050 m and 7.050 m from the detonation point. From the simulation, the results show that the blast pressure reduce from 136.34 kPa at 11.51 msec (inside of the building) to 134.02 kPa at 16.02 msec (outside of the building). Figure 4.8 shows the blast vector propagation with RC wall. At 0 msec, the pressure is at 101 kPa in atmospheric pressure. At 1.20 msec, the blast wave start to move. At 11.20 msec, the figure show that the blast vector start to hit the building. At 16.02 msec, the blast wave occupied the air domain.
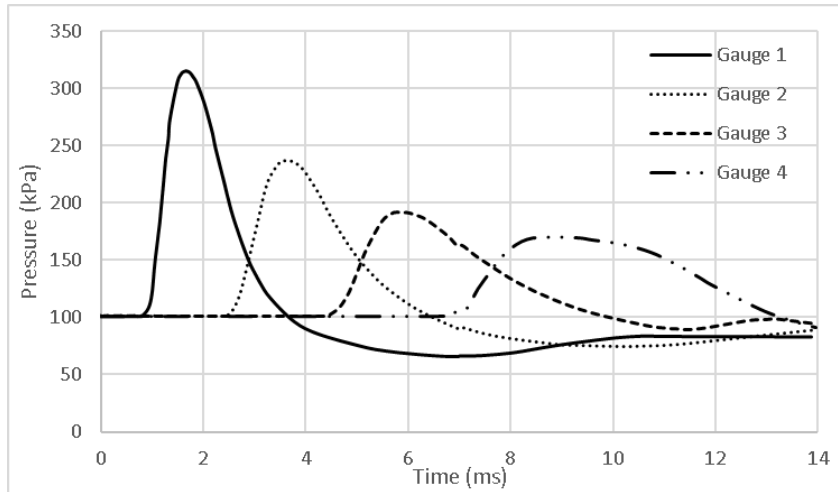
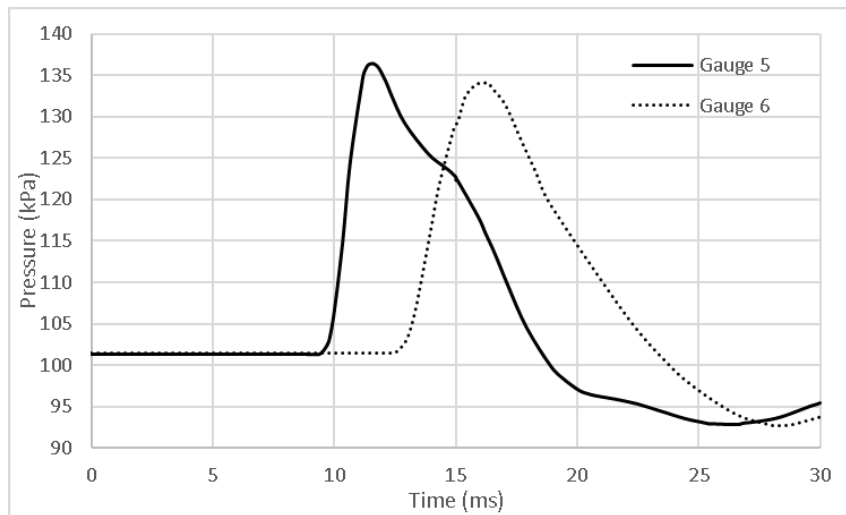Figure 4.6 Blast pressure parameter with RC wall

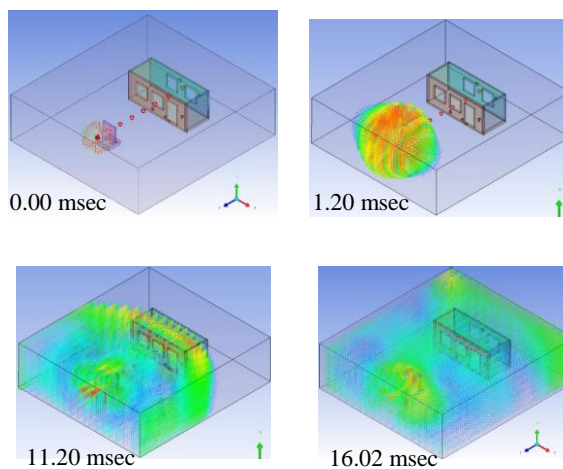Figure 4.7 Blast pressure parameter inside and outside of the building with RC wall

Figure 4.8 Blast vector propagation without RC wall

4.3   Discussion

From the blast pressure analysis in AUTODYN, it shows that the blast wedge (30 lbs TNT) was remapped in air volume Type 1 can be used for air volume Type 2 and air volume Type 3. The blast pressure recorded from simulation for free field shows that, it had similar peak blast pressure with blast test recorded by Yan et. al (2011) at 494.4 kPa at time 4.62 msec for free field and 494.4 kPa at time 4.64 msec. So, from the result it show that, the blast wedge 30 lbs TNT was valid to use for other parameter. From Table 4.1, it shows that with the presence of RC wall as barrier the blast pressure at distance 1.219 m from detonation point was reduced from 1255.63 kPa at 0.22 msec to 315.24 kPa at 1.66 msec. The percentage difference was about 120% when there is wall. The blast pressure also reduced at the distance 2.438 m, 3.657 m and 4.500 m from 458.30 kPa to 236.61 kPa, 264.36 kPa to 191.77 kPa and 233.26 kPa to 170. 43 kPa. The blast pressure inside of the house also reduced from 156.37 kPa to 136.34 kPa. The percentage difference was about 14% when RC wall act as barrier. From the simulation, it shows that if there was human living inside the building, that person would died because possible pressure that human can only stand was about 6.90 kPa based on Table. When human body was hit with this pressure, it would only cause light injuries from fragments.

Table 4.1 Comparison for peak blast pressure

Pressure Transducer	Blast overpressure without RC wall (kPa)	Blast overpressure with RC wall (kPa)	Percentage Difference %
1	1255.63	315.24	120
2	458.3	236.61	64
3	264.36	191.77	32
4	233.26	170.43	31
5	156.37	136.34	14
6	122.35	134.02	9

4.4   Summary

From the various type simulation conducted, the result was recorded as blast pressure (kPa) against time (msec) in various distance. The blast 30 lbs TNT in simulation was use in other parameter after it validated with blast test recorded by Yan et. al (2011) show similar blast peak pressure of 494.4 kPa at 6.24 msec. The highest blast pressure recorded was 1255.63 kPa at 0.22 msec. The result was recorded in air volume Type 2 without the presence of RC wall as barrier. When the blast pressure simulated with the presence of RC wall, the blast pressure reduced to 315.24 kPa at 1.66 msec. the percentage difference was about 120%. From the overall result recorded in simulation it shows that, the overall blast pressure was reduced when there was presence of RC wall as barrier. Although from the simulation shows that human cannot live inside of the building because the blast pressure was to high, it shows that the RC wall is very effective to use as barrier.

CHAPTER 5

CONCLUSION AND RECOMMENDATION

5.1   Conclusion

From the research study and simulation conducted, it can be conclude that through the numerical analysis of blast pressure parameters on the building with RC wall and without RC wall subjected to 30 lbs TNT as the following :

1. From the numerical analysis done in AUTODYN 3D FE, the result shows that the blast pressure will be reduced when there is RC wall as barrier compared to when there is no RC wall.

2. The numerical result show that RC wall is effective to use as barrier to reduced blast wave when there is blast occurred near the building

3. From the result recorded by numerical modelling, it shows that if there was human inside the building, the human will die either there were RC wall or not because the blast pressure recorded inside the building was very high for human body wo withstand.

4. From the analysis, it shows that the blast 30 lbs TNT use in this study was quite high.

5.2   Recommendation

Below recommendation for future research and simulation:

1. The blast use in the study must be lower TNT weight because 30 lbs had very high impact on building and also human. To know either human can survive if there were inside the building lower TNT weight was suggested to use as future study.

2. More RC wall should be added as fence for the building to ensure that when there explosion occurred near the building RC wall can absorb more blast pressure.

REFERENCES

Blast, S. (2012) 'Ship Blast Introduction to ANSYS AUTODYN', pp. 1–30.

Encyclopedia Britannica. (2019). *Trinitrotoluene | chemical compound*. [online] Available at: https://www.britannica.com/science/trinitrotoluene [Accessed 16 Jun. 2019].

Green, D. W., Winandy, J. E. and Kretschmann, D. E. (1917) 'Mechanical properties of wood determined', *Science*, 46(1195), pp. 516–517. doi: 10.1126/science.46.1195.516-a.

Gao, F. (2015) 'Numerical simulation of the droplet-surface impact using interfoam', (August). Available at: https://repository.library.northeastern.edu/files/neu:rx915z808/fulltext.pdf.

Hadden, B. J. D., Johann, M. a and Meacham, B. J. (2007) 'Blast Events', (January), pp. 38–41.

Koccaz, Z., Sutcu, F. and Torunbalci, N. (2008) 'Architectural and Structural Design for', *October*, (Figure 1).

Lethbridge, P. (2007) 'For Customers & Prospects', (October), pp. 1–37.

Ma, T., Xu, X. and Ning, J. (2017) 'Research on propagation laws of explosion shock wave inside metro station', *Journal of Loss Prevention in the Process Industries*. Elsevier Ltd, 46, pp. 54–68. doi: 10.1016/j.jlp.2017.01.009.

Malekan, M., Khosravi, A. and Cimini, C. A. (2019) 'Deformation and fracture of cylindrical tubes under detonation loading: A review of numerical and experimental analyses', *International Journal of Pressure Vessels and Piping*. Elsevier Ltd. doi: 10.1016/j.ijpvp.2019.05.003.

Nyström, U. and Gylltoft, K. (2009) 'Numerical studies of the combined effects of blast and fragment loading', *International Journal of Impact Engineering*, 36(8), pp. 995–1005. doi: 10.1016/j.ijimpeng.2009.02.008.

Pineda, S., Marongiu J. , Aubert S. and Lance M . (2019) 'Simulation of a gas bubble compression in water near a wall using the SPH-ALE method', *Computers and Fluids*. Elsevier Ltd, 179, pp. 459–475. doi: 10.1016/j.compfluid.2018.10.025.

Robertson, N., Hayhurst, C. and Fairlie, G. (1994) 'Numerical simulation of impact and fast transient phenomena using AUTODYN^{TM}-2D and 3D', *Nuclear Engineering and Design*, 150(2–3), pp. 235–241. doi: 10.1016/0029-5493(94)90140-6.

Remennikov, A. (2007) 'The state of the art of explosive loads characterisation', pp. 1–25.

Romick, C. M. and Aslam, T. D. (2017) 'High-order shock-fitted detonation propagation in high explosives', *Journal of Computational Physics*. Elsevier Inc., 332, pp. 210–235. doi: 10.1016/j.jcp.2016.11.049.

Strike, B. (2012) 'Bird Strike Introduction to ANSYS AUTODYN'.

So, A. K. W. and Chan, S. L. (1996) 'Nonlinear finite element analysis of glass panels', *Engineering Structures*, 18(8), pp. 645–652. doi: 10.1016/0141-0296(95)00199-9.

Shih-Ho, C. (2019). *How building design changed after 9/11*. [online] The Conversation. Available at: https://theconversation.com/how-building-design-changed-after-9-11-64580 [Accessed 13 Jun. 2019].

Yusof, M.A., Szer, L.W., Nor, N.M., Ismail, A., Yahya, M.A. and Peng, N.C., 2014. Simulation of Annealed Glass Panels Subjected to Air Blast Loading. , 4(8), pp.430–434.

Yan, D. Yin. H, Wu. C, Li Y, Baird J. and Chen J. (2016) 'Blast response of full-size concrete walls with chemically reactive enamel (CRE)-coated steel reinforcement', *Journal of Zhejiang University-SCIENCE A*, 17(9), pp. 689–701. doi: 10.1631/jzus.a1600480.

Zipf, R. K., Kenneth, P. E. and Cashdollar, L. (2010) 'Explosions and Refuge Chambers: Effects of blast pressure on structures and the human body'. Available at: https://www.cdc.gov/niosh/docket/archive/pdfs/NIOSH-125/125-ExplosionsandRefugeChambers.pdf.